JOURNAL OF GUIDANCE, CONTROL, AND DYNAMICS
Vol. 19, No. 1, January–February 1996

Control of a Flexible Beam Using Back Electromotive Force of Motor

Hironori A. Fujii, Shinji Hatano, and Khoichi Matsuda
Tokyo Metropolitan Institute of Technology, Tokyo 191, Japan

An innovative method of wave-absorbing control is presented for vibration suppression of flexible space structures. The method needs no digital computation process programmed under the control law that is usually necessary in realistic systems. A torque motor is used not only as an actuator but also a sensor that detects the angular velocity of the motor shaft, and the control loop is closed without digital computation. The control approach is to treat the vibration as superposed wave modes traveling in positive and negative directions and to suppress the outgoing wave modes at the actuator position. The motor is connected to the electric circuit that has a frequency-dependent impedance and constitutes a compensator. The back electromotive force of the motor is generated by the rotation of the motor shaft and is put into the electric circuit to generate electric current. The torque of the motor that is generated by the current is adapted to the wave-absorbing controller. The performance of the present method is verified through both numerical simulation and experiments.

I. Introduction

LARGE-SPACE structures (LSS) will be so flexible that they can easily be excited in their structural vibration. It is important to establish a control method of LSS vibration suppression for LSS to realize satisfactory performance, and active vibration control in LSS has been given considerable notice in the past decades. The most usual method employs a dynamic model that is described by discretized parameters for such distributed parameter systems as flexible structures. Methods not employing discretization process are, however, essentially natural and well suited to control flexible structures free from the crucial truncation effect.

Wave-absorbing control is one of the control methods that needs no discretization process. The traveling wave approach for the control of LSS is presented by von Flotow and Schäfer[1] and by von Flotow.[2] Reference 1 introduces the viewpoint that the response of a flexible structure can be explained with the disturbance propagation characteristics of the structure. The control method aims to suppress the wave modes excited elsewhere in the structure by

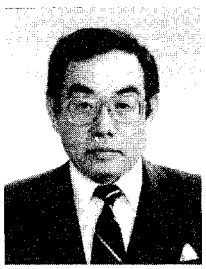

Hironori A. Fujii is a Professor in the Department of Aerospace Engineering at the Tokyo Metropolitan Institute of Technology. He earned his D.E. degree in 1975 from Kyoto University. His research interests include dynamics and control of large space structures and robotics for aerospace application. Since 1982 he has been responsible for the coordination of the Research Group on Control of Flexible Space Structures in Japan. He is an Associate Fellow of AIAA, a member of the American Astronautical Society and the Japan Society for Aeronautical and Space Sciences, and an Associate Fellow of the Canadian Aeronautics and Space Institute.

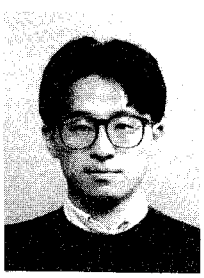

Shinji Hatano is a graduate student in the master's program of the Tokyo Metropolitan Institute of Technology. He received his undergraduate degree in aerospace engineering in 1994 from the Tokyo Metropolitan Institute of Technology. His research interests include dynamics and control of large space structures. He is a Student Member of the Japan Society for Aeronautical and Space Sciences.

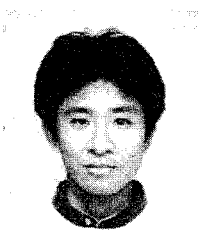

Khoichi Matsuda received the B.E. and M.E. degrees in Aerospace Engineering in 1991 and 1993, respectively, from the Tokyo Metropolitan Institute of Technology. He is currently working towards the Ph.D. degree in Aerospace Engineering at the same institute. His current research interests include dynamics and control of distributed parameter systems. He is a Student Member of AIAA and the Japan Society for Aeronautical and Space Sciences.

Received Jan. 18, 1994; revision received May 29, 1995; accepted for publication June 13, 1995.

canceling the wave propagation. Active damping of vibration by canceling traveling waves is studied in Refs. 3–6. Control methods for vibration suppression are introduced, such as the vibration isolation in Ref. 3, independent modal-space control method and direct feedback control in Ref. 4, and active control in a supposed waveguide in Ref. 5. Experiments are also demonstrated in Ref. 6 that verify the validity of the wave-absorbing control method for vibration suppression of flexible structures modeled as a hinged-free beam with a noncollocated controller. It is shown in these studies that the transfer function of an ideal controller contains irrational terms that can be realized approximately over finite bandwidth. The present paper studies analytically, numerically, and experimentally a method of wave-absorbing control for vibration suppression of flexible structures using the back electromotive force (emf) of a motor, and partial differential equations are employed to express the structural dynamics for the controller design.

There are several methods for estimating and controlling the states of an electromagnetic actuator.[7–10] Sensorless active control of magnetic bearings is studied in Ref. 7, but this control method does not seem to work well because the position is estimated from the voltage shift of the coil. Sensorless active vibration control is proposed in Refs. 8–10, where an active vibration control method is designed through the use of a moving coil type electromagnetic actuator as a two-port sensing and driving device. It is a well-known and interesting fact that the electromagnetic actuator has another function as a sensor, i.e., the back emf is produced in the actuator in proportion to the velocity of the move of the actuator. Thus, it is possible to use the actuator as a velocity sensor simultaneously by employing the back emf of the motor. Velocity feedback control of the linear actuator is proposed in Refs. 8 and 9, and the estimation of the disturbance torque in dc drive is introduced in Ref. 10 using the classical observer theory. These studies report the applications of the relation between the velocity of the movement and the back emf of the actuator. In the present study, the control law is implemented by an electric circuit and the control loop is closed without using the process of digital computation. The back emf of a motor is used in an active manner as a sensor that detects the angular velocity of the motor shaft.

The present control method can work well to suppress the vibration of flexible structures by the employment of the wave-absorbing control method through the use of the back emf of the motor. The validity of the control method is verified through both numerical simulation and an experiment conducted on a hinged-free beam model.

II. Controller Design

We apply the traveling wave approach techniques used by von Flotow and Schäfer[1] to analyze the behavior of a flexible beam. The system model is illustrated in Fig. 1. The predominant flexibility of a beam is assumed to have horizontal deflections, $w(x,t)$, in only one plane, where x is the spatial coordinate and t time. The behavior of the beam deflections is described by the following partial differential equation (damping and tensile forces are ignored):

$$\rho A\frac{\partial^2 w(x,t)}{\partial t^2}+EI\frac{\partial^4 w(x,t)}{\partial x^4}=F(x,t) \tag{1}$$

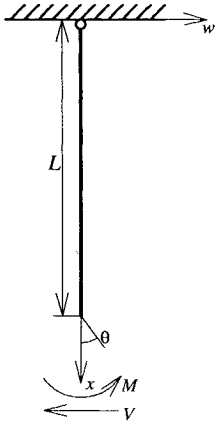

Fig. 1 Model configuration; hung hinged-free flexible beam model.

together with the boundary conditions

$$w(0,t)=0 \tag{2a}$$

$$EI\frac{\partial^2 w}{\partial x^2}(x,t)=M_C(t) \tag{2b}$$

$$EI\frac{\partial^2 w}{\partial x^2}(L,t)=0 \tag{2c}$$

$$EI\frac{\partial^3 w}{\partial x^3}(L,t)=0 \tag{2d}$$

where E is Young's modulus, I the cross-sectional moment of inertia, ρ the mass density of the beam, and L the length of the beam. The control force $F(x,t)$ does not include the control torque M_C applied at the root of the beam.

The partial differential equation, Eq. (1), is Laplace transformed as follows (to avoid new symbols, the transformed variables hereafter have the same notation as their time-dependent equivalents):

$$\rho As^2 w(x,s)+EI\frac{\partial^4 w}{\partial x^4}(x,s)=F(x,s) \tag{3}$$

and the beam dynamics of Eq. (3) are described by

$$\frac{\mathrm{d}\boldsymbol{y}}{\mathrm{d}x}=\begin{bmatrix}0&1&0&0\\0&0&\frac{1}{EI}&0\\0&0&0&1\\-\rho As^2&0&0&0\end{bmatrix}\boldsymbol{y}+\begin{bmatrix}0\\0\\0\\F(x,s)\end{bmatrix} \tag{4}$$

with the introduction of the cross-sectional state vector $\boldsymbol{y}=[w\ \theta\ M\ V]^T$, where $\theta=\partial w/\partial x$ is the slope, $M=EI(\partial\theta/\partial x)=EI(\partial^2 w/\partial x^2)$ is the internal bending moment, and $V=\partial M/\partial x=EI(\partial^3 w/\partial x^3)$ is the internal shear force.

It is convenient to set $F(x,s)=0$ in Eqs. (3) and (4) to describe the separate processes of wave propagation and wave generation by the external force.

Equation (4) is diagonalized by the transformation

$$\boldsymbol{y}=\begin{bmatrix}1&1&1&1\\i\lambda&\lambda&-i\lambda&-\lambda\\-M_0&M_0&-M_0&M_0\\-iV_0&V_0&iV_0&V_0\end{bmatrix}\boldsymbol{u}=\boldsymbol{Y}(s)\boldsymbol{u} \tag{5}$$

where $i=\sqrt{-1}$, $\lambda=\sqrt[4]{(-s^2\rho A/EI)}=\sqrt[4]{(\rho A/EI)}(1-i)\sqrt{(s/2)}$, $M_0=\lambda^2 EI$, and $V_0=\lambda E_0$.

The cross-sectional state vector $\boldsymbol{u}=[a_1\ a_2\ b_1\ b_2]^T$ is ordered, where a_1 and a_2 are the amplitudes of wave modes traveling toward the lower end of the beam and b_1 and b_2 are wave modes departing the lower end of the beam. These wave modes consist of frequency-dependent combinations of physical cross-sectional state variables and the columns of the matrix $\boldsymbol{Y}$, and they are independent one another along the beam. The amplitudes of these wave modes vary according to the relation

$$\frac{\mathrm{d}\boldsymbol{u}}{\mathrm{d}x}=\begin{bmatrix}i\lambda&0&0&0\\&\lambda&0&0\\&&-i\lambda&0\\\mathrm{sym}&&&-\lambda\end{bmatrix}\boldsymbol{u} \tag{6}$$

and the solution of the Eq. (6) is described as

$$a_1=C_1e^{i\lambda(s)x} \tag{7a}$$

$$a_2=C_2e^{\lambda(s)x} \tag{7b}$$

$$b_1=C_3e^{-i\lambda(s)x} \tag{7c}$$

$$b_2=C_4e^{-\lambda(s)x} \tag{7d}$$

The displacement of the beam is represented by the superposition of four wave modes

$$w = a_1 + a_2 + b_1 + b_2$$
$$= C_1 e^{i\lambda x} + C_2 e^{\lambda x} + C_3 e^{-i\lambda x} + C_4 e^{-\lambda x} \quad (8)$$

It is clear from these equations that a_1 and b_1 are the amplitudes of the traveling wave, and also a_2 and b_2 decay exponentially with x.

To analyze the beam dynamics at the root of the beam in wave-mode coordinates, the boundary conditions for the state vector $\boldsymbol{y}$ at $x = 0$ and the externally applied (control) torque M_C are introduced in matrix form:

$$\begin{bmatrix} 1 & 0 & 0 & 0 \\ 0 & 0 & 1 & 0 \end{bmatrix} \boldsymbol{y}(0, s) = \begin{bmatrix} 0 \\ M_C(s) \end{bmatrix} \quad (9)$$

and are transformed into wave-mode coordinates through the use of Eq. (5):

$$\begin{bmatrix} 1 & 1 & 1 & 1 \\ -M_0 & M_0 & -M_0 & M_0 \end{bmatrix} \boldsymbol{u}(0, s) = \begin{bmatrix} 0 \\ M_C(s) \end{bmatrix} \quad (10)$$

Partitioning $\boldsymbol{u}(0, s)$ into incoming waves a_j and outgoing waves b_j and inversion of a 2×2 matrix leads to the result

$$\begin{bmatrix} b_1 \\ b_2 \end{bmatrix} = \begin{bmatrix} 0 & -1 \\ -1 & 0 \end{bmatrix} \begin{bmatrix} a_1 \\ a_2 \end{bmatrix} + \begin{bmatrix} -\dfrac{1}{2M_0} \\ \dfrac{1}{2M_0} \end{bmatrix} M_C(s) \quad (11)$$

or, in general,

$$\boldsymbol{b}(0, s) = \boldsymbol{S}\boldsymbol{a}(0, s) + \boldsymbol{B}M_C \quad (12)$$

It is seen from Eq. (11) that the outgoing wave modes $\boldsymbol{b}(0, s)$ are produced by the reflection of the incoming wave modes $\boldsymbol{a}(0, s)$ and are generated by control torque $M_C(s)$. The reflection coefficient matrix $\boldsymbol{S}$ of the incoming wave modes shows that the phase of the outgoing waves shifts π rad from that of the incoming waves.

The wave-absorbing controllers are designed through use of Eq. (11) but are limited to the following form in this experiment:

$$M_C(s) = C(s)s\theta \quad (13)$$

where the control torque $M_C(s)$ is applied in response to the angular velocity of the shaft of the motor, $\dot{\theta}$. The closed-loop scattering behavior at the root of the beam is obtained from Eqs. (11) and (13) as follows:

$$\boldsymbol{b}(0, s) = \boldsymbol{S}_{\mathrm{CL}}\boldsymbol{a}(0, s) \quad (14)$$

where $\boldsymbol{S}_{\mathrm{CL}}(s)$ is the closed-loop scattering matrix

$$\boldsymbol{S}_{\mathrm{CL}} = \{\boldsymbol{I} - \boldsymbol{B}C(s)s[-i\lambda \quad -\lambda]\}^{-1}\{\boldsymbol{S} + \boldsymbol{B}C(s)s[i\lambda \quad \lambda]\}$$
$$= \frac{Cs\lambda}{2M_0 + (1-i)Cs\lambda} \times \begin{bmatrix} -\dfrac{2M_0}{Cs\lambda} - (1+i) & -2 \\ 2i & -\dfrac{2M_0}{Cs\lambda} + (1+i) \end{bmatrix} \quad (15)$$

In the case that the controller $C(s)$ that leads to $\boldsymbol{S}_{\mathrm{CL}} = \boldsymbol{0}$ exists, it is clear from Eq. (14) that the outgoing wave modes $\boldsymbol{b}(0, s)$ are not generated by any incoming waves $\boldsymbol{a}(0, s)$. In the present formulation of the control problem, all elements of $\boldsymbol{S}_{\mathrm{CL}}$, however, cannot be set zero at same time for all frequency ranges. The control algorithm is thus set to nullify the element of $\boldsymbol{b}$ as much as possible. From this viewpoint, $C(s)$ that leads to $\det \boldsymbol{S}_{\mathrm{CL}} = 0$ is selected as follows:

$$C(s) = -\sqrt{\frac{2}{-i}\frac{M_0}{s\lambda}} = \frac{2EI}{\sqrt{s}}\sqrt[4]{\frac{\rho A}{EI}} \quad (16)$$

It may seem preferable to set $C(s) = 2M_0/\{(1+i)s\lambda\}$, which leads to $S_{\mathrm{CL}}(1, 1) = 0$. The element of the matrix $S_{\mathrm{CL}}(1, 1)$ is the reflection coefficient of predominant importance, since it describes generation of the outgoing traveling wave modes by the incident traveling wave modes. The derived controller, however has a problem for implementation in that it includes an imaginary number. The present controller is to be realized by an electric circuit using a back emf of a motor, and it is generally difficult to realize a controller whose transfer function contains imaginary numbers. Thus, the alternative selection is employed to set $\det \boldsymbol{S}_{\mathrm{CL}} = 0$. If the determinant of $\boldsymbol{S}_{\mathrm{CL}}$ is set to zero, it is obvious that a rank of $\boldsymbol{S}_{\mathrm{CL}}$ is 1, and there exists a nonzero $\boldsymbol{a}$ such that $\boldsymbol{S}_{\mathrm{CL}}\boldsymbol{a} = \boldsymbol{0}$. The present controller is able to suppress the outgoing wave mode corresponding to the specified condition of $\boldsymbol{a}$. Through this approach, both of the outgoing waves, the traveling wave mode b_1 and the wave mode of the near fields b_2, are taken into account for cancellation, although the compensator does not completely cancel the whole outgoing wave.

III. Hardware Setup

Figure 2 shows the hardware setup of an experimental model used in this study. As shown in Fig. 2a, the stainless-steel beam is suspended vertically from a support structure to allow free vibration in the vertical plane, with the upper end fixed to the shaft of a dc torque motor and the lower end free. The dc torque motor is an actuator to control reflection of traveling waves at its position and is a sensor of angular velocity using the back emf of the motor.

Figure 2b shows the components of the electric circuit that is used in this study. The motor at the upper end of the beam is connected as one of the resistors of the Wheatstone bridge circuit. The back emf is produced in proportion to the angular velocity of the shaft of the motor. If the motor generates back emf, an electric potential difference occurs between two edges of the bridge circuit. The output of the bridge circuit is extracted by a differential amplifier being restricted to the low-frequency range through use of a low-pass filter (LPF) and is put into the half-integrator ($1/\sqrt{s}$) circuit to realize the controller, Eq. (16), electrically. There are two ac amplifiers to complete the controller, except for the half-integrator. By passing through the circuit, the back emf is transformed into electric current, and by feeding the electric current into the Wheatstone bridge, the motor generates torque that suppresses the angular velocity of the motor. To avoid the self-inductive electromotive force caused by the reverse of the input current to the motor, another coil of the motor is added in the opposite side of the bridge. A variable resistance is set in order to adjust the balance of the bridge.

Disturbance is applied to the flexible structure in order to identify the beam dynamics. The source of the disturbance is given by a driver, whose link is rotated by a dc torque motor. A current pulse drives the dc torque motor to apply random force to the beam at the position near to the tip of the beam, and the current pulse is generated by a digital computer.

IV. Electric Realization of Compensator

In this study, the control method described in Sec. II is installed using an analog electric circuit. All resistors, condensers, and operational amplifiers used in the circuit are commercially available

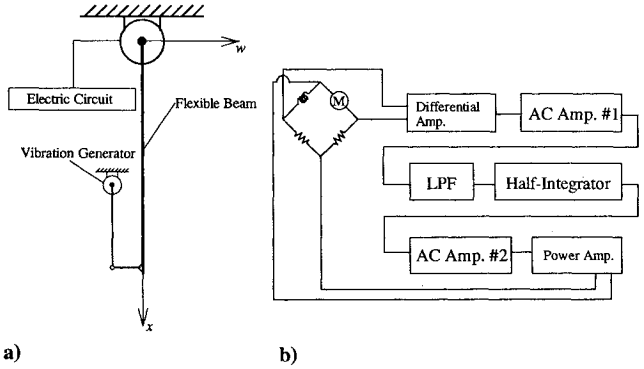

a) b)

Fig. 2 Hardware setup: a) experimental model and b) components of the electrical circuit used in the experiment.

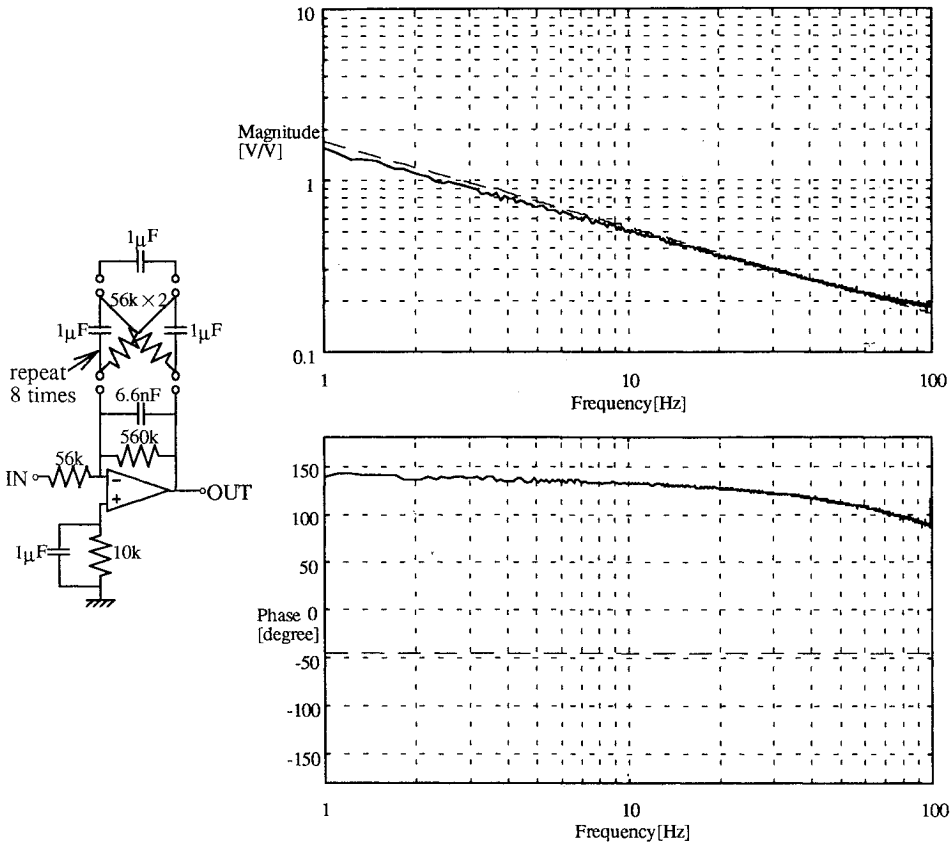

Fig. 3 Half-integrator circuit and its measured performance; random voltage input at in-terminal, measurement at out-terminal: solid line, measurement values; broken line, numerical simulation.

devices. To improve accurate performance of the circuit, the operational amplifiers in the main division are selected from a viewpoint that the chips should have no internal noise and no voltage drift caused by thermal changes and passage of time. The operational amplifiers used in this experiment are OP-07 and OP-27G (Precision Monolithics Inc.). The laminated ceramic condensers are selected such that the electric charge and discharge are completed in sufficiently short time.

A circuit that yields a $1/\sqrt{s}$ behavior has been introduced[1] that is shown in Fig. 3, together with its performance measured experimentally. The performance is based on the well-known fact that the characteristic impedance of an R–C lattice is $1/\sqrt{(sRC)}$. In this case, the impedance is $4.23/\sqrt{s}$. To implement a half-integrator, a resistor is used as the input impedance of the operational amplifier, and the desired behavior is most closely obtained at 17.9 Hz. The gain is set to follow very closely the $4/\sqrt{s}$ frequency behavior, as shown in Fig. 3, where the performance is studied using numerical simulation. The gain is seen to agree well with that of the numerical simulation, whereas the phase is deviated from the ideal one considerably. The phase of output shifts about π rad in the limited frequency from 1 to 30 Hz. This is because an inverting amplifier is employed as an amplification component of the circuit, and the experimental circuit needs another inverting amplifier to correct the phase.

Several operational amplifiers are used in the circuit in this study. Every operational amplifier has an offset voltage in output and thus has offset null terminals to avoid the effect of the offset voltage. The offset voltage, however, varies with the transition of package temperature that is caused by heat creation of the amplifier and thermal change of the environment. A high degree of tolerance is required in the output because the gain of the circuit is about 700.

Figure 4 shows a circuit that only amplifies alternating currents, and the circuit is divided into three components. The first component is an alternative current connection that is used to eliminate the direct current ingredient due to the condenser. The second component is a noninverted amplifier circuit. The third component is a first-order high-pass filter (HPF). The cutoff frequency both of the alternative current connection and HPF is set to 0.884 Hz. The circuit amplifies

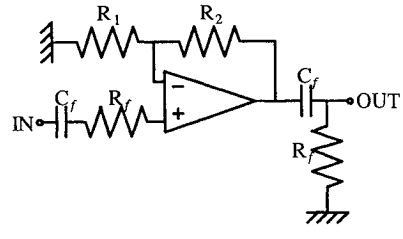

Fig. 4 Alternating current amplifier; a schematic diagram and relations between factors of elements. Cutoff frequency $f_c = 1/2\pi C_f R_f$; $|V_{OUT}|/|V_{IN}| = 1 + (R_2/R_3)$.

the alternative current signal and eliminates the offset voltage of its input.

V. Experimental Results

The experimental setup has already been described in Sec. III; details of the bridge circuit are explained in this section. The flexible beam is equipped with two dc torque motors as the controller and the shaker, which are commercially available devices (LC38-188 Copal, Japan). Table 1 shows the parameters of the stainless-steel beam and the motor used in the numerical simulation and the experiment. These parameters of the motor are determined experimentally. It is noted that the moment of inertia of the rotor of the motor can be ignored because it is $1/(2.34 \times 10^7)$ that of the beam, even if the rotor is assumed to be a simple cylinder with same weight as the original one.

The nominal values in the catalog of the motor gives the relationship of the current passed through the motor I_M (in amperes) to the angular velocity N_M (in radians per second), and the generated torque M_M (in newton meters):

$$N_M = 545.6 - 185.3 I_M \tag{17a}$$

$$M_M = 4.112 \times 10^{-2} I_M - 4.876 \times 10^3 \tag{17b}$$

Table 1 Parameters of the experimental hardware

Stainless steel beam	
Thickness, m	0.001
Width, m	0.03
Length, m	2.0
Bending rigidity EI, N·m^2	5.15×10^{-1}
Mass per unit length of the beam ρ, kg/m	2.40×10^{-1}
Motor	
Internal electric resistance of the motor R_M, Ω	8.3
Ratio of the back emf to angular velocity of the shaft k_b, V/(rad/s)	4.48×10^{-2}

Table 2 Parameters of the circuit

Gain of the alternative current amplifier 1	10
Gain of the alternative current amplifier 2	x
Multiplying factor of the half-integrator circuit	4.23
Conversion factor of the power amplifier, A/V	0.51
Resistors of the Wheatstone bridge, Ω	$R_C = 8.3$
	$R_1 = R_2 = 10$

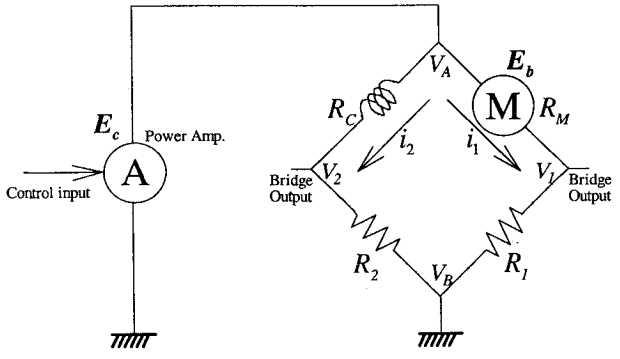

Fig. 5 Several variables in the bridge circuit.

It is known that the relationship of the back emf to the angular velocity of the shaft is described as follows:

$$E_b = k_b\dot{\theta} = 4.48 \times 10^{-2} \times \dot{\theta} \tag{18}$$

As illustrated in Fig. 5, several variables are designed to construct the bridge circuit. If the bridge circuit is balanced well (to meet with the requirement $R_M/R_1 = R_C/R_2$), the electric potential difference is produced in proportion to the back emf as follows:

$$V_1 - V_2 = \frac{R_M}{R_M + R_1} E_b \tag{19}$$

The output of the experimental circuit illustrated in Fig. 2b is given by

$$I_{\text{out}}(s) = 0.51 \frac{4.23 \times 10 \times x}{\sqrt{s}} \frac{R_M}{R_M + R_1} E_b \tag{20}$$

Table 2 shows the parameters for the components of the experimental circuit in Fig. 2 necessary to represent Eq. (20).

The following relations hold at the bridge circuit shown in Fig. 5:

$$I_{\text{out}} = i_1 + i_2 \tag{21a}$$

$$V_A - V_B = (R_M + R_1)i_1 + E_b = (R_C + R_2)i_2 \tag{21b}$$

From Eqs. (21a) and (21b), the relation between the input current for the bridge I_{out} and the input current for the motor I_M is given as follows:

$$I_M = \frac{(R_C + R_2)I_{\text{out}} - E_b}{R_M + R_C + R_1 + R_2} \tag{22}$$

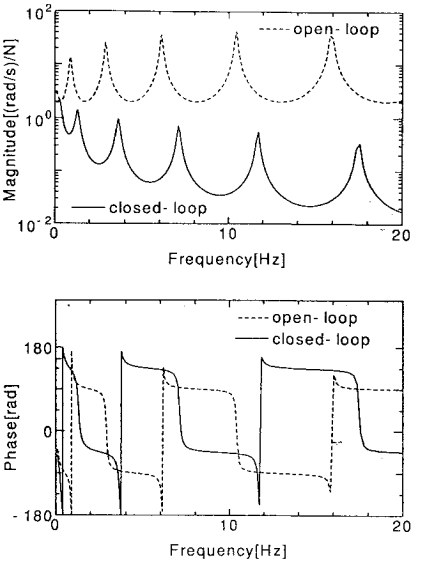

Fig. 6 Numerically calculated open- and closed-loop structural responses; random force excitation at the tip; angular velocity measurement at the root.

The control torque led by the angular velocity of the shaft is derived from Eqs. (17b), (18), (20), and (22) as follows:

$$M_C = \frac{-4.112 \times 10^{-2}}{R_M + R_C + R_1 + R_2}\left(21.57 R_M \frac{R_C + R_2}{R_M + R_1}\frac{x}{\sqrt{s}} - 1\right) \times k_b s\theta - 4.876 \times 10^{-3} \tag{23}$$

Neglecting small terms in Eq. (23), we obtain

$$M_C = \frac{8.870 \times 10^{-1} \cdot R_M}{R_M + R_C + R_1 + R_2} \frac{R_C + R_2}{R_M + R_1} \frac{x}{\sqrt{s}} k_b s\theta \tag{24}$$

Comparing Eqs. (13) and (16) with Eq. (24), the gain of the alternative current amplifier 2 is selected to be $x = 66.69$.

The transfer function of the controller, Eq. (16), can be realized approximately over a finite bandwidth. The control law is implemented by an electric circuit, and its performance is verified through numerical simulation. Results of the numerical simulation are shown in Fig. 6 with the transfer functions of the structural responses both for the open- and closed-loop cases. It is seen that the present control method works well to suppress vibration of the flexible structure by employing the wave-absorbing control method through the use of the back emf of the motor.

Experimental results are shown in Fig. 7 where the behavior is observed from the output of the alternative current amplifier 1 in the experimental circuit. Good vibration suppression is clearly observed from these results by the present control experiment. A few reasons for the difference between the simulation and the experiment are noted here as follows.

1) Several peaks of gain are seen in the closed-loop response in Fig. 7 approximately at 8.4, 13.2, and 17.8 Hz. The peaks are the vibration of the beam torsion inherent in the experiment model, which do not appear in the results of the numerical simulation. These peaks are not seen in the open-loop response because of the much higher gain in the 5 ~ 20 Hz frequency.

2) A difference in the phase of closed loop is seen between the numerical simulation and the experimental result. The phase of the compensator circuit cannot be matched perfectly to the ideal compensator, because the alternating current amplifiers shift the phase of input signal considerably. Further, the output voltage of the bridge circuit increases impulsively every time the direction of the torque applied to the upper end of the beam is inverted. The impulses of voltage have such considerable effect as the undesirable torque is applied to the upper end of the beam.

3) The measured open-loop structural response in the frequency less than about 1 Hz is smaller in magnitude than that of the numerical simulation because the hanging beam in the experiment

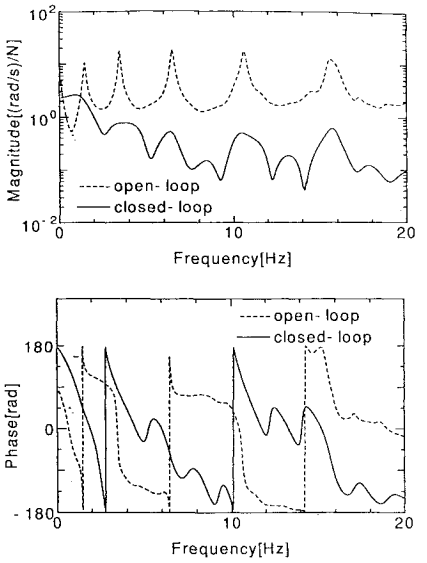

Fig. 7 Experimentally obtained open- and closed-loop structural responses; random force excitation at the tip; angular velocity measurement at the root.

can be considered to be strengthened due to the effect of the gravity. Note that the pendulum mode at about 0.5 Hz that is dominant in the experiment results are caused by gravity. These results show a limitation of on-ground experimentation of flexible space structures.

4) Since the gain of the experimental circuit amounts to about 700 times, the circuit amplifies not only essential signals but noises as well. It is extremely difficult to eliminate the noises from outputs of the electric circuits that have the large amplifier gain without loss of preciseness.

In the course of the experiment, it is seen that the value of the resistors in the bridge circuit varies due to the effect of the thermal change. A cemented wire-wound resistor has durability against high electric power and, at the same time, has considerable error caused by the effect of thermal change. These cemented resistors in the bridge had warmed up during the experiment. The resistance value of the rheostat in the bridge circuit also fluctuates affecting the result of the experiment. These facts make the regulation of the circuit difficult, and improvements of the characteristics of the resistors and the rheostat are recommended, if better performance of the controller is wanted for further realistic applications.

VI. Conclusions

A wave-absorbing control method to suppress vibration of a flexible structure using the back emf of a motor whose shaft is fixed to the end of the beam is studied in this paper. The control approach is to treat the vibration as superposed wave modes traveling in positive and negative directions and to suppress the outgoing wave modes at the actuator position. The controller is implemented approximately in an electric circuit with frequency-dependent impedance. The half-integrator $(1/\sqrt{s})$ is implemented in the controller and is approximately realized by the use of the circuit that includes R–C lattice network. The back emf of the motor is generated by the rotation of the motor shaft and is put into the electric circuit to generate electric current. The torque of the motor that is generated by the current is adapted to the wave-absorbing controller. The motor is used not only as an actuator to suppress the vibration of the flexible beam but also as a sensor to detect the angular velocity of actuating point using the back emf. It is shown both numerically and experimentally that the present innovative control method can be applied successfully without using digital computation. The present paper is regarded as one of the ways to implement the control method for vibration suppression with a collocated controller and is expected to find many applications for flexible vibration control without having to employ the discretized mathematical model and without having to use the digital computer, for example, for control of large space structures and flexible robot arm.

Acknowledgments

The authors wish to thank T. Ohtsuka and H. Hatakenaka for helpful discussions and suggestions.

References

[1]Von Flotow, A. H., and Schäfer, B., "Wave-Absorbing Controllers for a Flexible Beam," *Journal of Guidance, Control, and Dynamics*, Vol. 9, No. 6, 1986, pp. 673–680.

[2]Von Flotow, A. H., "Traveling Wave Control for Large Spacecraft Structures," *Journal of Guidance, Control, and Dynamics*, Vol. 9, No. 4, 1986, pp. 462–468.

[3]McKinnell, R. J., "Active Vibration Isolation by Canceling Bending Waves," *Proceedings of the Royal Society of London*, Vol. A421, 1989, pp. 357–393.

[4]Benninghof, J. K., and Meirovitch, L., "Active Suppression of Traveling Waves in Structures," *Journal of Guidance, Control, and Dynamics*, Vol. 12, No. 4, 1989, pp. 555–567.

[5]Mace, B. R., "Active Control of Flexural Vibration," *Journal of Sound and Vibration*, Vol. 114, No. 2, 1987, pp. 253–270.

[6]Fujii, H. A., and Ohtsuka, T., "Experiment of a Noncollocated Controller for Wave Cancellation," *Journal of Guidance, Control, and Dynamics*, Vol. 15, No. 3, 1992, pp. 741–745.

[7]Vischer, D., and Bleuler, H., "A New Approach to Sensorless and Voltage Controlled AMBs Based on Network Theory Concepts," *Proceedings of the 2nd International Symposium on Magnetic Bearings* (Tokyo, Japan), Inst. of Industrial Science, Univ. of Tokyo, Japan, 1990, pp. 301–306.

[8]Hashitani, H, Okada, Y., and Nagai, B., "Sensorless Active Vibration Control (Moving Coil as an Actuator and Velocity Sensor)," *Journal of the Japan Society of Mechanical Engineers* (C), Vol. 58, No. 554, 1992, pp. 2912–2917 (in Japanese).

[9]Okada, Y., Hashitani, H., Zhang, H., and Tani, J., "Electromagnets as Velocity Sensors and Vibration Control Actuators," *Proceedings of the 3rd International Symposium on Application of Electromagnetic Forces* (Sendai, Japan), Elsevier, Tokyo, Japan, 1991, pp. 171–174.

[10]Buja, G. S., Menis, R., and Valla, M. I., "Disturbance Torque Estimation in a Sensorless dc Drive," *Proceedings of the 19th International Conference on Industrial Electronics, Control, and Instrumentation* (Maui, HI), Inst. of Electrical and Electronics Engineers, Computer Society Press, Los Alamitos, CA, 1993, pp. 977–982.